



# Measurement of $e^+ e^- \rightarrow K\bar{K}$ cross section via ISR method

---

Hua Shi<sup>1</sup>, Yijing Wang<sup>1</sup>, Huiliang Xia<sup>1</sup>, Tiantian Lei<sup>1</sup>, Dong Liu<sup>1</sup>, Weiping Wang<sup>2</sup>,  
Dexu Lin<sup>3</sup>, Achim Denig<sup>2</sup> and Guangshun Huang<sup>1</sup>

<sup>1</sup>University of Science and Technology of China

<sup>2</sup>Johannes Gutenberg University Mainz

<sup>3</sup>Institute of Modern Physics, CAS

第十届BESIII R值与QCD强子结构研讨会

2025年7月28日 乌鲁木齐



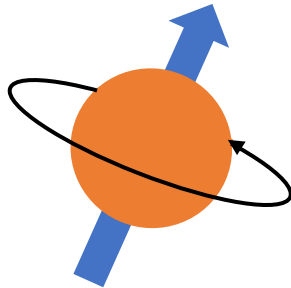


# Outline

---

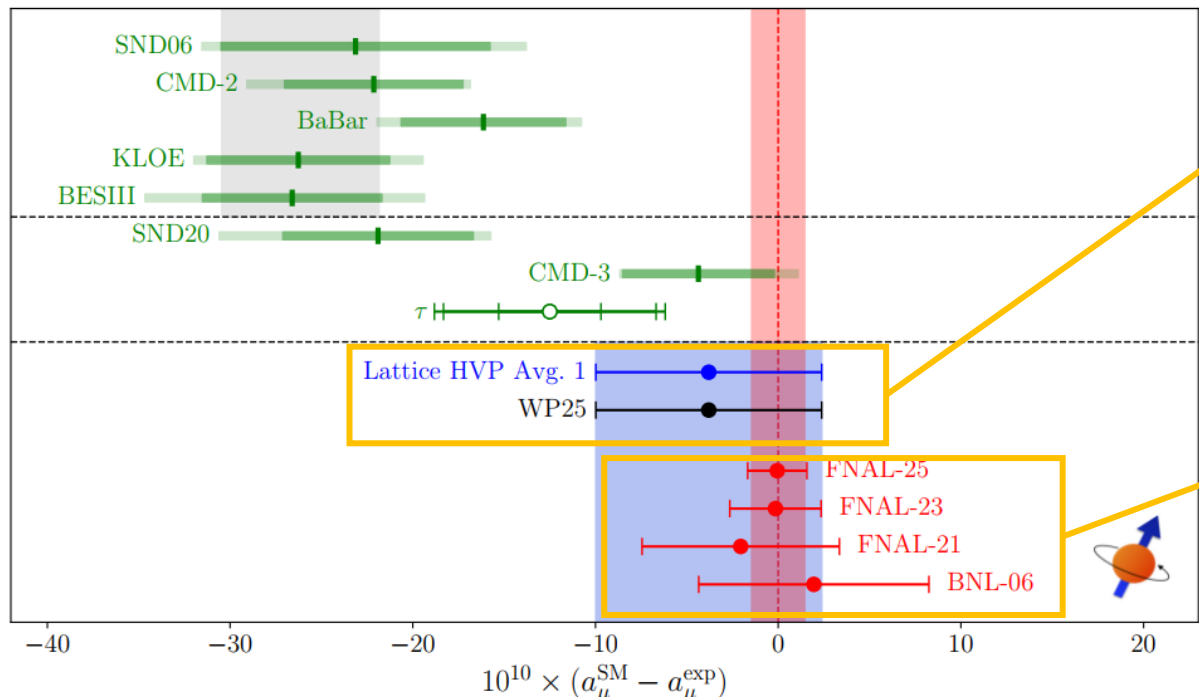
- Motivation
- BESIII Experiment: Advantage
- Initial State Radiation Method
- $K\bar{K}$  Cross Section
- Summary

# Motivation



- The anomalous magnetic moment of muon ( $a_\mu = (g - 2)_\mu/2$ )

- The Dirac equation predicts a muon magnetic moment:  $\vec{M} = g \frac{e}{2m_\mu} \vec{S}$  with  $g = 2$
- Magnetic anomaly to evaluate the deviation:  $a_\mu \equiv \frac{g-2}{2}$

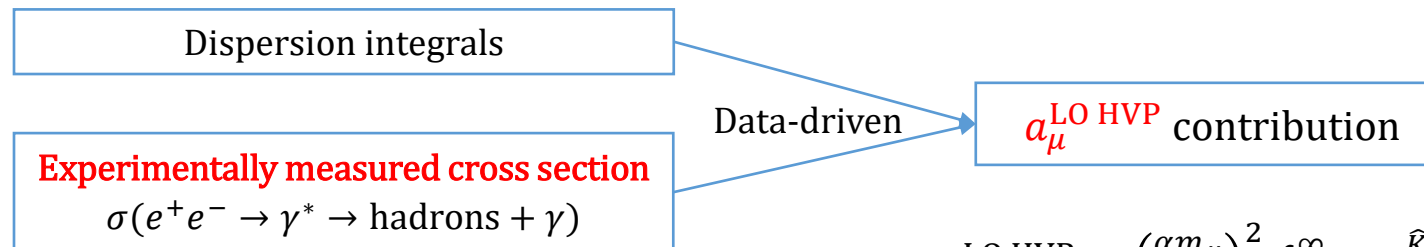


arXiv: 2505.21476

- Updated Standard Model prediction in WP25:  $a_\mu^{\text{SM}}$
- ✓ Most important development since WP20: estimation of leading-order hadronic-vacuum-polarization (LO HVP) contribution, **Data-driven → Lattice QCD calculation**
- Experimental measurement:  $a_\mu^{\text{exp}}$
- ✓ Brookhaven National Lab (BNL)
- ✓ Fermilab (FNAL)
- No tension between  $a_\mu^{\text{SM}}$  and  $a_\mu^{\text{exp}}$  at the current precision
- Precision of  $a_\mu^{\text{SM}}$  must be improved by about a factor of four to match the one of  $a_\mu^{\text{exp}}$

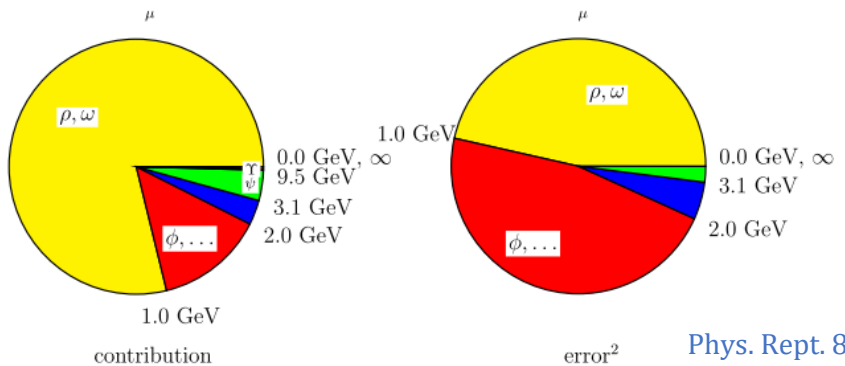
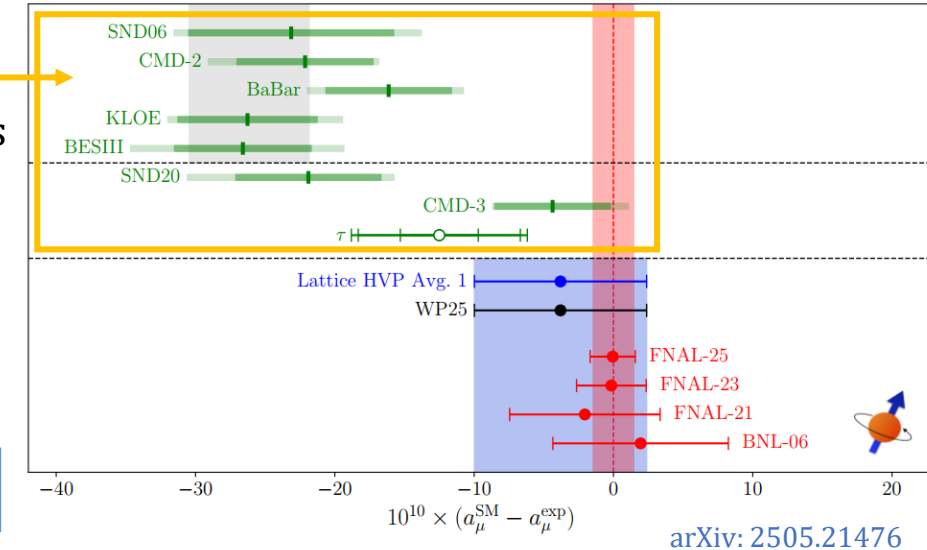
# Motivation

- Why lattice calculation used here?
  - Significant **deviations** in data-driven results among different collaborations
  
- How to understand these deviations and what can we do?
  - An improved understanding of **higher-order radiative corrections**



$$a_\mu^{\text{LO HVP}} = \left( \frac{\alpha m_\mu}{3\pi} \right)^2 \int_{s_{\text{thr}}}^\infty ds \frac{\hat{K}(s)}{s^2} R_{\text{had}}(s), R_{\text{had}}(s) = \frac{\sigma[e^+e^- \rightarrow \text{hadrons}(\gamma)]}{4\pi\alpha^2/(3s)}$$

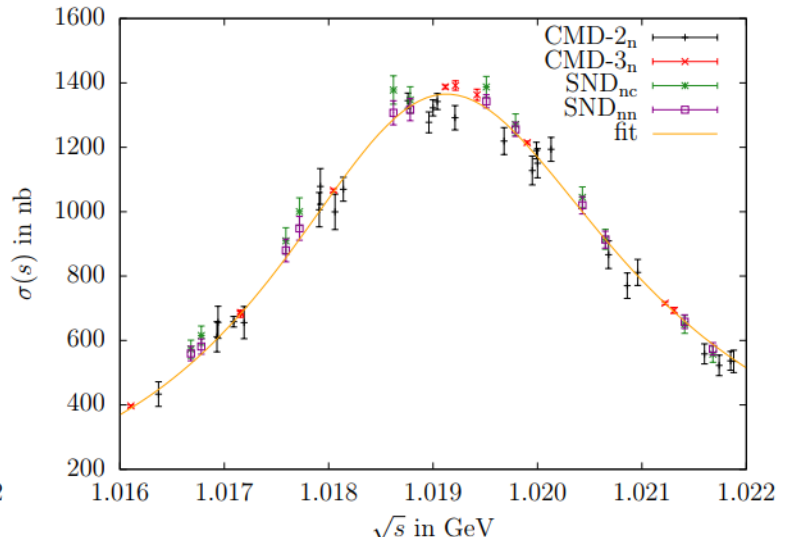
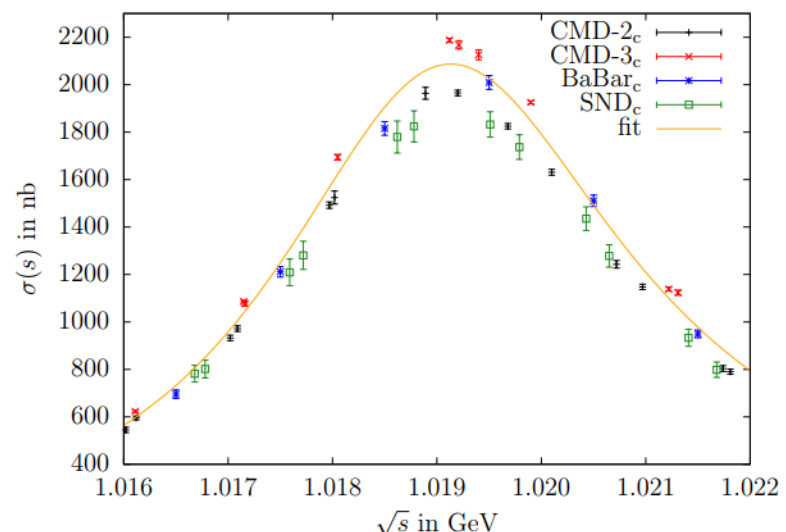
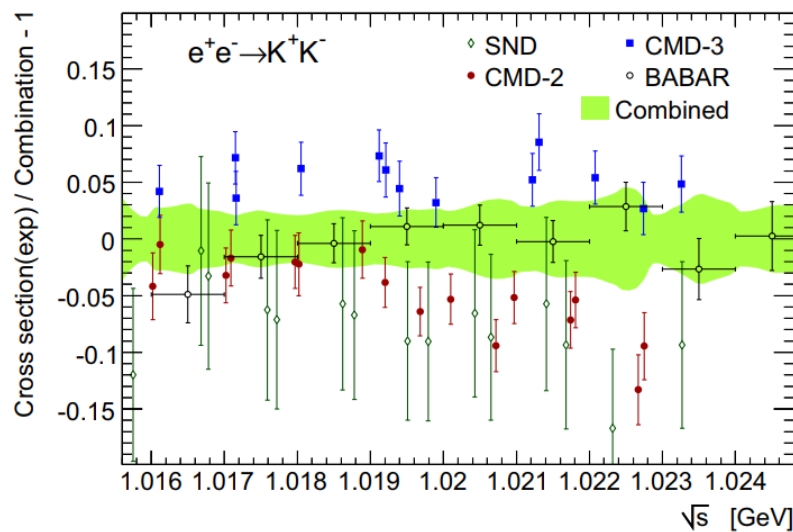
- More **precise measurements**
  - I.  $\lesssim 2$  GeV: exclusive final states ( $2\pi, 3\pi, 4\pi, 2K(K^+K^-, K_SK_L), \dots$ )  
 inclusive  $R$  value via ISR or energy scan method
  - II.  $\gtrsim 2$  GeV: inclusive hadronic  $R$  value



# Motivation

- Discrepancies between data from different experiments in  $KK$  channel
  - Tensions observed in  $K^+K^-$  channel around  $\phi$  peak, not clear in  $K_SK_L$  channel

arXiv: 2505.21476  
 Phys. Rept. 887, 1-166 (2020)  
 Eur. Phys. J. C 80,241 (2020)

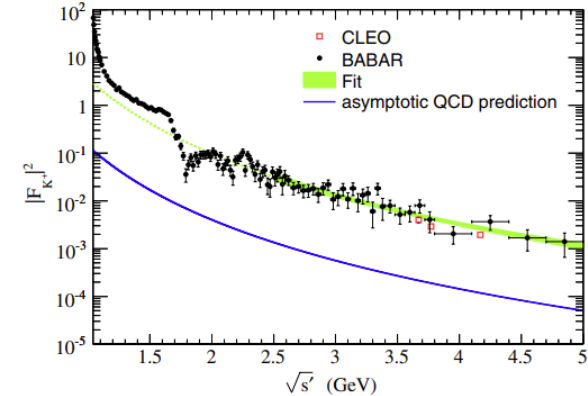


- More accurate cross section measurement around  $\phi$  peak are needed

# Motivation

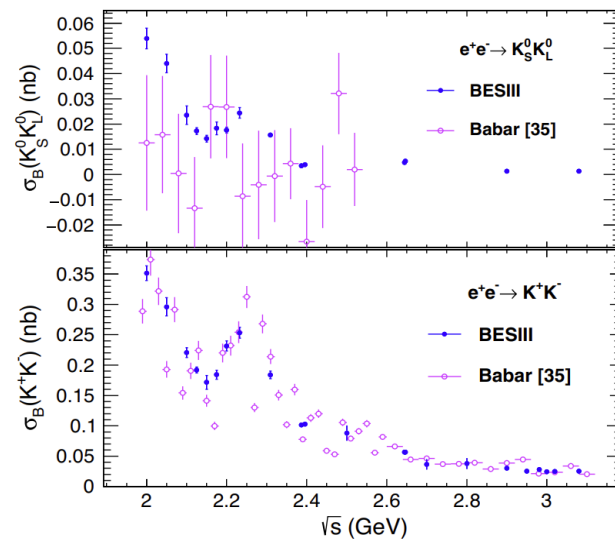
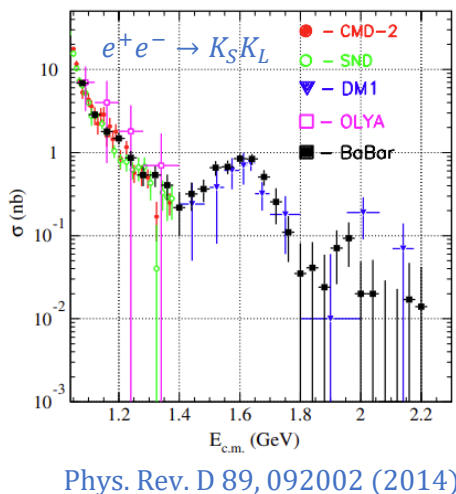
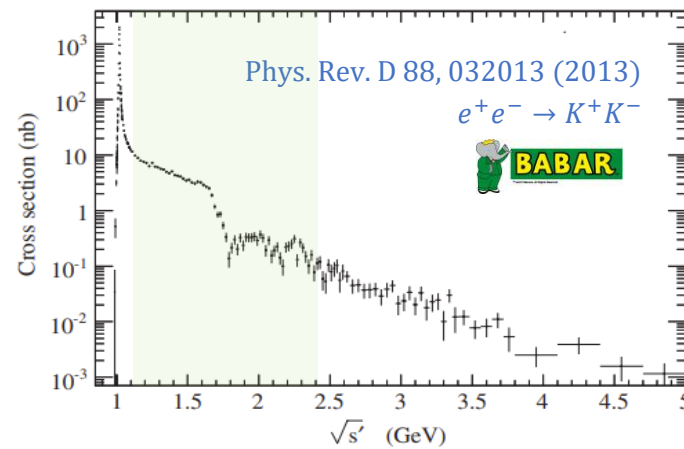
## ➤ Kaon electromagnetic form factor

- Direct insight into the distribution of charges, currents, color and flavor
- Charged Kaon form factor:
  - Energy-dependent form factor at higher-energy data is consistent with the asymptotic form predicted by pQCD
  - Their magnitude is about 4 times higher than the predicted asymptotic value
- How about neutral Kaon?



Phys. Rev. D 104, 092014(2021)  
Phys. Rev. D 99, 032001 (2019)

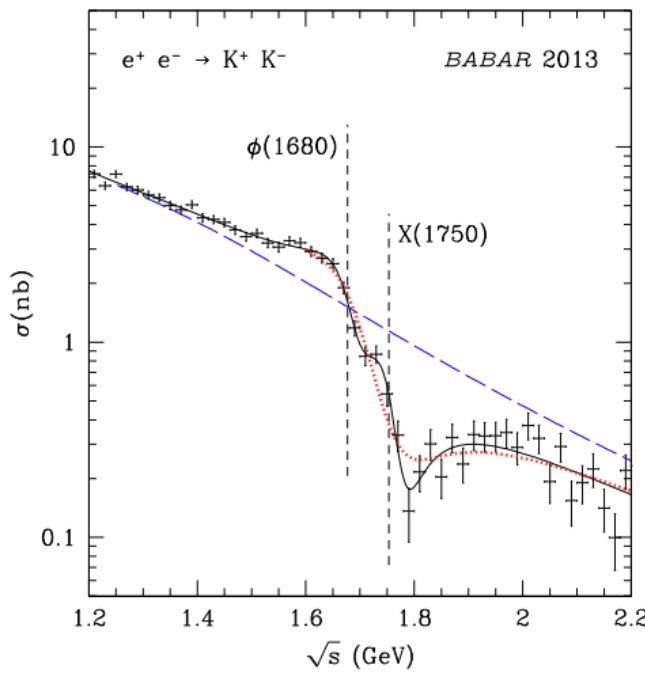
## ➤ Substantial structures are evident in the center-of-mass energy range 1.1 – 2.4 GeV



# Motivation

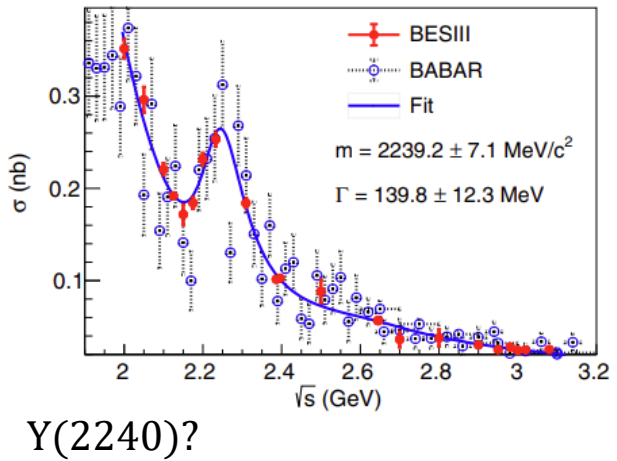
- Provide more information about the vector resonances

? Can the  $X(1750)$  be a  $\phi(1750)$ ?

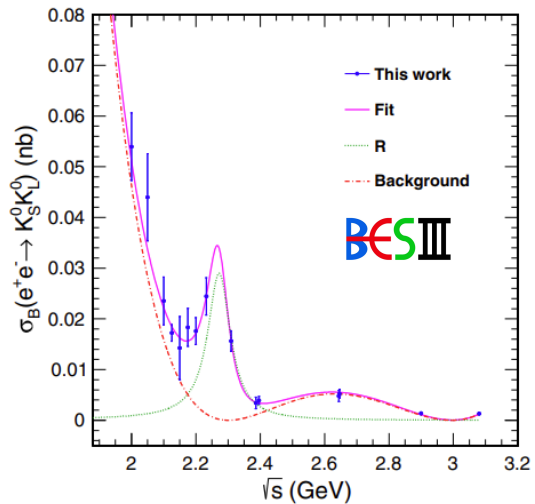
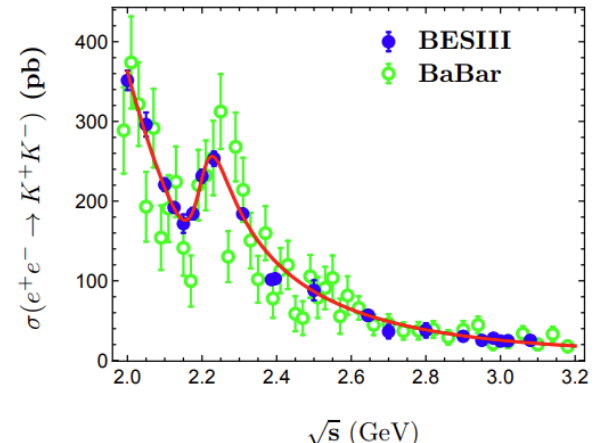


Phys. Rev. D 111, L071903(2025)

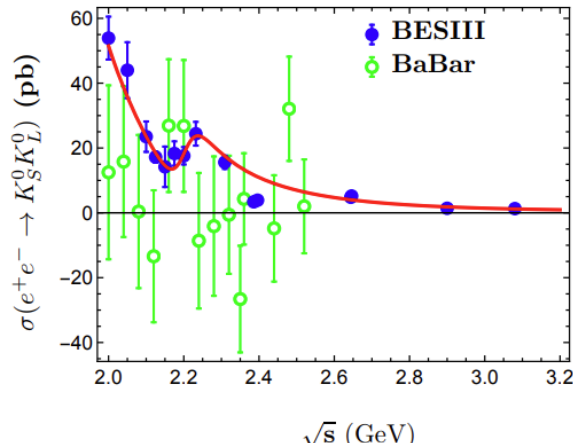
?  $\phi(2170)$ ?



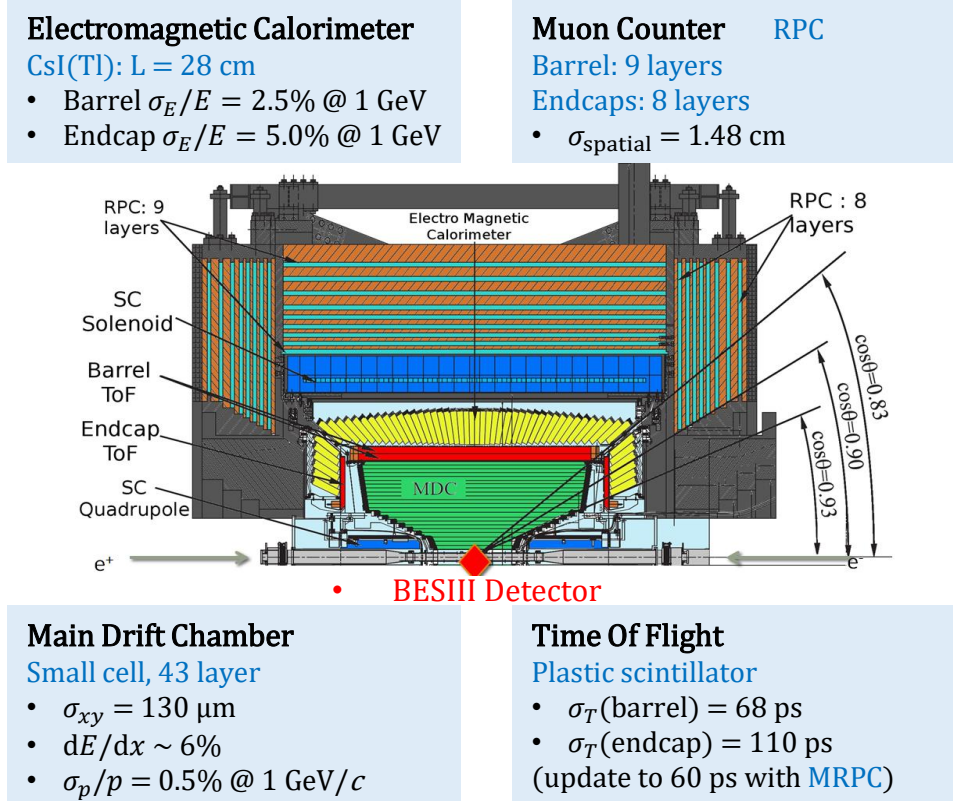
?  $Y(2240)$ ?



arXiv: 2504.18797

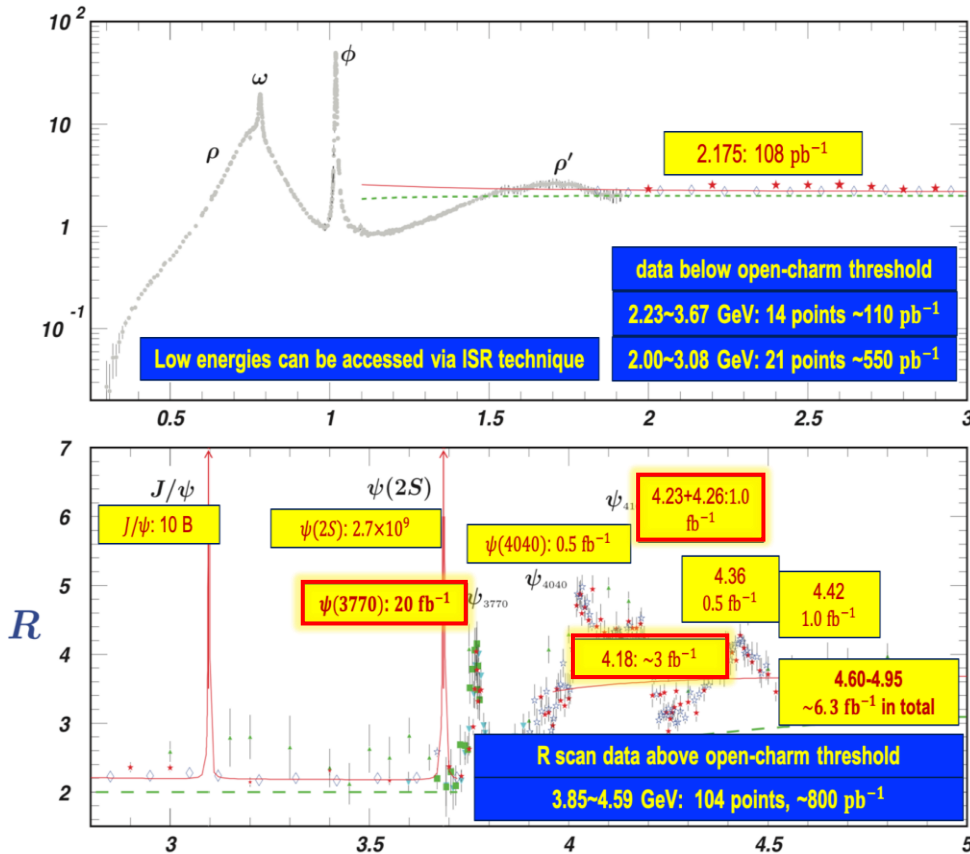


# BESIII Experiment: Advantages



- ✓ Symmetric  $e^+e^-$  collisions
- ✓ Good resolution
- ✓ High detection efficiency
- ✓ Lower background

Nucl. Instrum. Meth. A 614, 345-399 (2010)



- ✓ Large datasets:  $20 \text{ fb}^{-1}$  at  $\psi(3770)$ ,  $10 \text{ fb}^{-1}$  at XYZ region
- ✓ **Ideal environment** to measure  $e^+e^- \rightarrow K\bar{K}$  cross section with initial state radiation method!
- ✓ Also for measurement by energy scan method

# Initial State Radiation(ISR) Method

## ➤ Initial State Radiation (ISR) Method at a fixed c.m. energy

- At a **fixed** c.m. energy  $\sqrt{s}$ , collecting events from **threshold to  $\sqrt{s}$**
- Systematic uncertainty in a **coherent** way
- Large luminosity needed
- **Higher** background than energy scan method

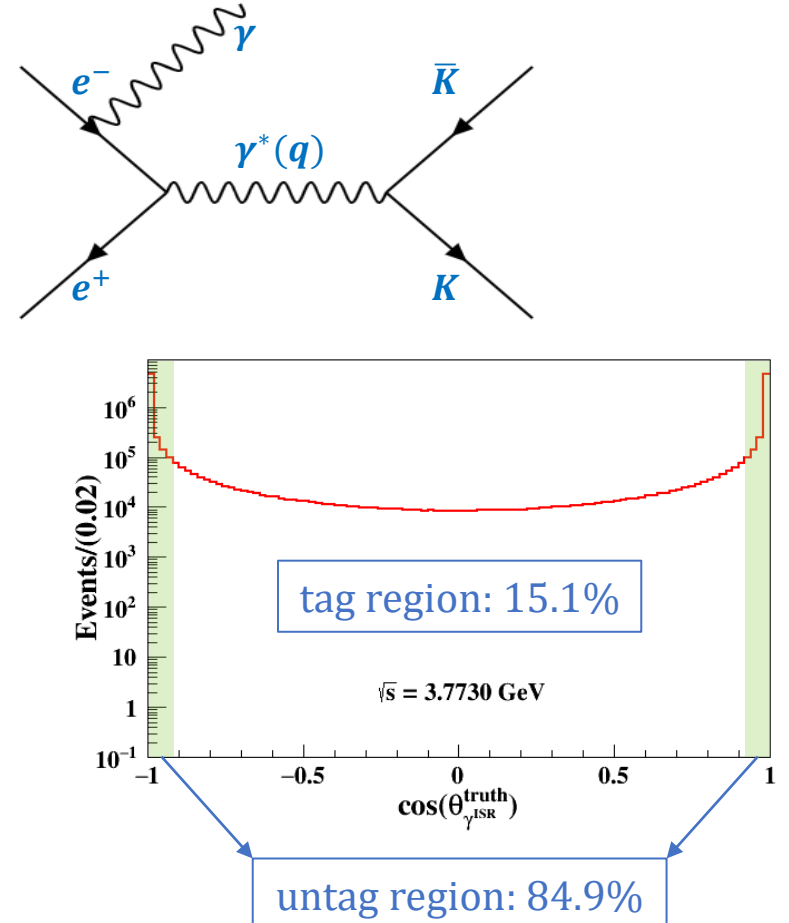
## ➤ Two reconstruction method

### I. Events with a tagged ISR photon (tag)

- ✓ From threshold → More contributions for  $a_\mu^{\text{LO HVP}}$
- ✗ Low reconstruction efficiency

### II. Events with an untagged ISR photon (untag)

- ✓ High reconstruction efficiency → better to explore structures in  $M(K\bar{K})$
- ✗ Can't start from threshold



✓ ISR photons emitted mainly along the direction of beam pipe

# $K\bar{K}$ cross section

➤ Datasets:

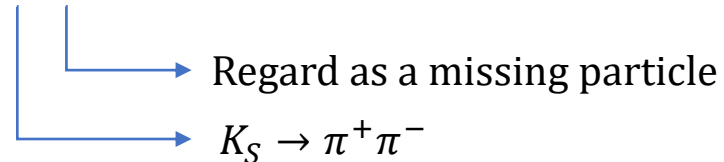
$\sqrt{s}$ (GeV)	$\mathcal{L}$ (fb $^{-1}$ )
3.773	20.3
4.008 ~ 4.157	1.3
4.178	3.2
4.189 ~ 4.288	6.1

➤ MC samples:

- Determine the detection efficiency
- Estimate the background contributions

➤ Analyses ongoing:

- $e^+e^- \rightarrow K^+K^-$  with a tagged ISR photon(tag  $K^+K^-$ )
- $e^+e^- \rightarrow K^+K^-$  with an untagged ISR photon(untag  $K^+K^-$ )
- $e^+e^- \rightarrow K_SK_L$  with a tagged ISR photon(tag  $K_SK_L$ )



Process	Generator	Samples	Process	Generator	Samples
$e^+e^- \rightarrow \gamma^{\text{ISR}} K^+K^-$	PHOKHARA	$\sim 11\times$	$e^+e^- \rightarrow \gamma^{\text{ISR}} J/\psi$	BesEvtGen	$\sim 40\times$
$e^+e^- \rightarrow \gamma^{\text{ISR}} K_SK_L$	PHOKHARA	$\sim 118\times$	$e^+e^- \rightarrow \gamma^{\text{ISR}} \psi(2S)$	BesEvtGen	$\sim 40\times$
$e^+e^- \rightarrow q\bar{q}$	KKMC/LundAreaLaw	$\sim 8\times$	$\gamma\gamma \rightarrow K^+K^-$	cppGamGam	$\sim 30\times$
$e^+e^- \rightarrow \psi(3770) \rightarrow \text{non-DD}$	KKMC+BesEvtGen	$\sim 40\times$	$\gamma\gamma \rightarrow \pi^+\pi^-$	GALUGA2.0	$\sim 1\times$
$e^+e^- \rightarrow \gamma^{\text{ISR}} \pi^+\pi^-$	PHOKHARA	$\sim 6\times$	$\gamma\gamma \rightarrow \mu^+\mu^-$	DIAG36	$\sim 1\times$
$e^+e^- \rightarrow \gamma^{\text{ISR}} e^+e^-$	BABAYAGA	$\sim 0.25\times$	$\gamma\gamma \rightarrow e^+e^-$	DIAG36	$\sim 2\times$
$e^+e^- \rightarrow \gamma^{\text{ISR}} \mu^+\mu^-$	PHOKHARA	$\sim 10\times$	$\gamma\gamma \rightarrow \eta$	EKHARA	$\sim 1\times$
$e^+e^- \rightarrow \gamma^{\text{ISR}} \tau^+\tau^-$	KKMC	$\sim 40\times$	$\gamma\gamma \rightarrow \eta'$	EKHARA	$\sim 1\times$

# Background Analysis Method

- Background level in each analysis

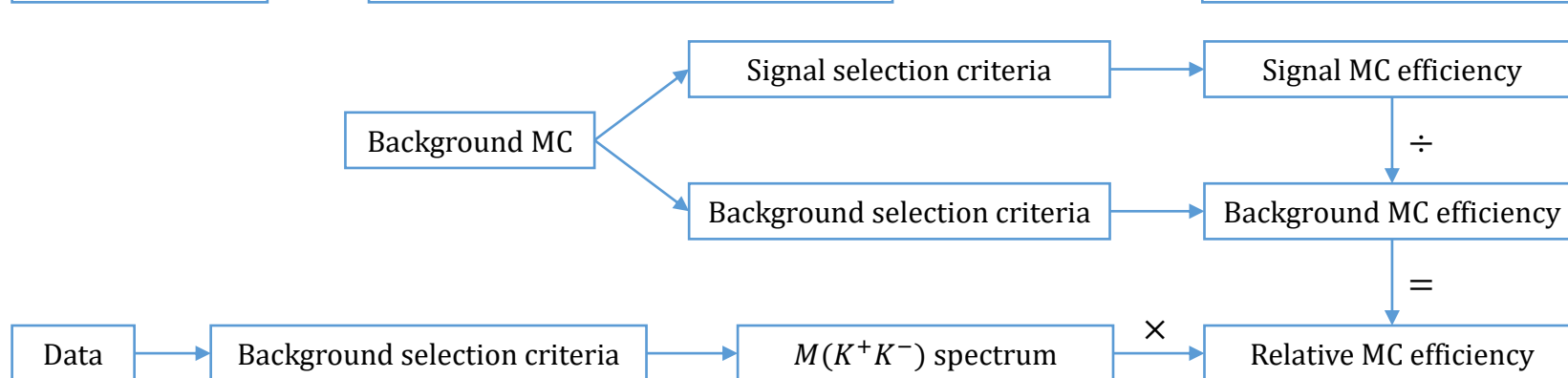
Analysis	tag $K^+K^-$			untag $K^+K^-$		tag $K_SK_L$	
$M(K\bar{K})$ region	$[M(K^+K^-)_{\text{th}}, 1.1]$	[1.1, 2.5]	[2.5, 3.0]	[1.2, 2.5]	[2.5, 3.2]	$[M(K_SK_L)_{\text{th}}, 1.1]$	[1.1, 2.0]
Background(%)	0.8	2.2	25.7	4.2	9.0	9.2	80.1

- How to estimate backgrounds

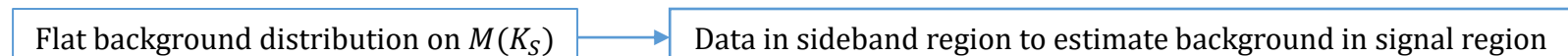
- MC estimation



- Data driven



- Sideband



# ISR Radiation Function

## ➤ Comparison between calculation and MC generator PHOKHARA

### ✓ Strategy:

- 20M  $e^+e^- \rightarrow \gamma^{\text{ISR}}\mu^+\mu^-$  MC, generated by PHOKHARA, NLO ISR enabled, FSR and VP switched off

Nucl. Phys. B 318, 1-21 (1989)

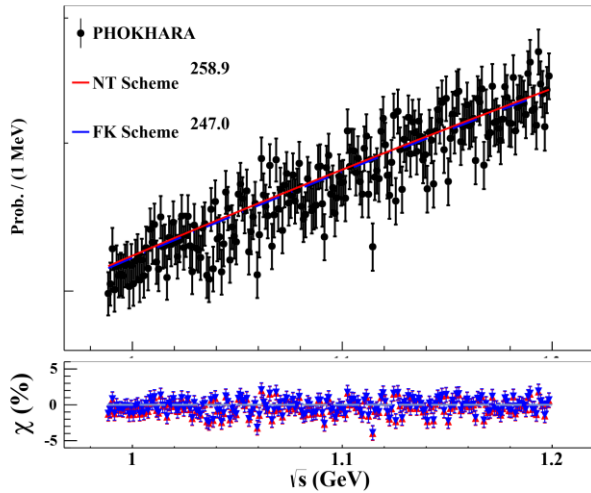
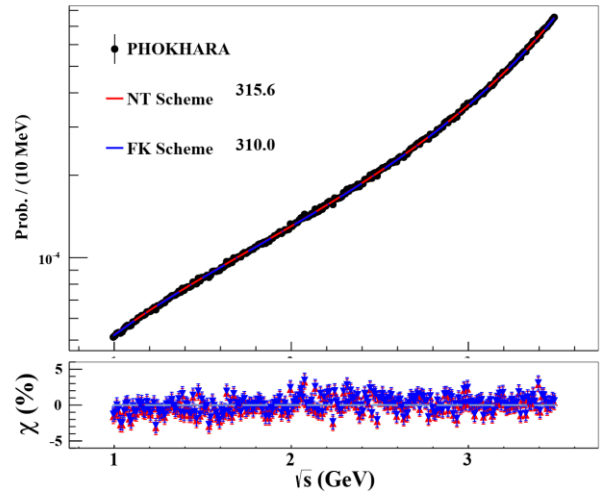
$$\frac{L_i}{L} = \frac{\sigma_i^{e^+e^- \rightarrow \gamma^{\text{ISR}}\mu^+\mu^-}}{\sigma_i^{e^+e^- \rightarrow \mu^+\mu^-}} \quad \sigma_{e^+e^- \rightarrow \mu^+\mu^-} = \frac{86.8}{s} \text{ nb}$$

### ✓ Function:

Used  $\leftarrow$

- $F_{SF}^{\text{FK}}(x, s) = \beta x^{\beta-1} \left[ 1 + \frac{\alpha}{\pi} \left( \frac{\pi^2}{3} - \frac{1}{2} \right) + \frac{3}{4} \beta - \frac{\beta^2}{24} \left( \frac{1}{3} L + 2\pi^2 - \frac{37}{4} \right) \right] - \beta \left( 1 - \frac{1}{2} x \right) - \frac{1}{8} \beta^2 \left[ 4(2-x)\ln x + \frac{1+3(1-x)^2}{x} \ln(1-x) + 6 - x \right]$   $\beta = 2\alpha(L-1)/\pi, L = \ln(s/m_e^2)$
- $F_{SF}^{\text{NT}}(x, s) = \beta x^{\beta-1} \Delta - \beta \left( 1 - \frac{1}{2} x \right) - \frac{1}{8} \beta^2 \left[ 4(2-x)\ln x + \frac{1+3(1-x)^2}{x} \ln(1-x) + 6 - x \right],$   
 $\Delta = 1 + \frac{\alpha}{\pi} \left( \frac{3}{2} L + \frac{\pi^2}{3} - 2 \right) + \left( \frac{\alpha}{\pi} \right)^2 \left\{ \left[ \frac{9}{8} - 2\zeta(2) \right] L^2 + \left[ -\frac{45}{16} + \frac{11}{2} \zeta(2) + 3\zeta(3) \right] L - \frac{6}{5} [\zeta(2)]^2 - \frac{9}{2} \zeta(3) - 6\zeta(2)\ln 2 + \frac{3}{8} \zeta(2) + \frac{57}{12} \right\}$

### ✓ Result:



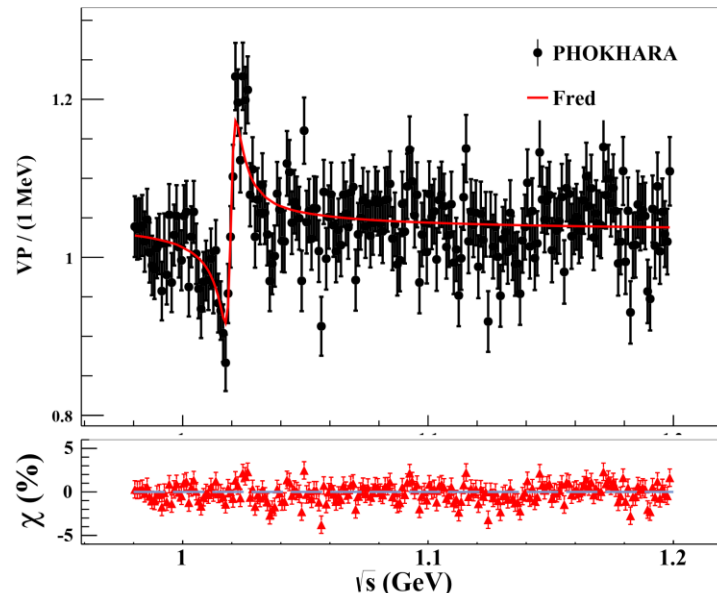
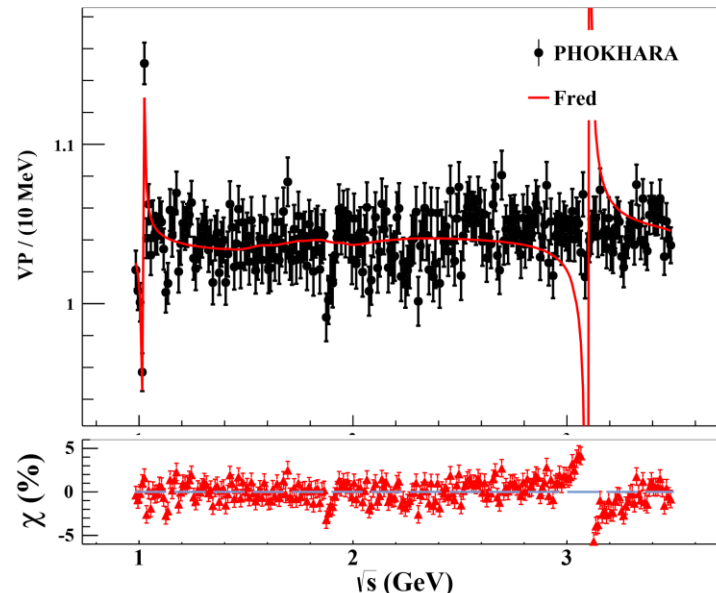
# Vacuum polarization

## ➤ Comparison between calculation and MC generator PHOKHARA

### ✓ Strategy:

- 10M  $e^+e^- \rightarrow \gamma^{\text{ISR}}\mu^+\mu^-$  MC, generated by PHOKHARA, NLO ISR and VP enabled, FSR switched off,  $J/\psi$  is excluded in MC generated
- $\frac{\sigma_i^{e^+e^- \rightarrow \gamma^{\text{ISR}}\mu^+\mu^-}}{\sigma_i^{e^+e^- \rightarrow \mu^+\mu^-}} = w(x, s) \cdot f_{\text{vp}}$        $\sigma_{e^+e^- \rightarrow \mu^+\mu^-} = \frac{86.8}{s}$  nb       $w(x, s) = F_{\text{SF}}^{\text{FK}}(x, s)$

### ✓ Result:





# $K\bar{K}$ cross section

## ➤ Resolution

Analysis	tag $K^+K^-$			untag $K^+K^-$		tag $K_SK_L$	
$M(K\bar{K})$ region	$[M(K^+K^-)_{\text{th}}, 1.1]$	[1.1, 2.5]	[2.5, 3.0]	[1.2, 2.5]	[2.5, 3.2]	$[M(K_SK_L)_{\text{th}}, 1.1]$	[1.1, 2.0]
Resolution	1 MeV(unfolding)	4 MeV	7 MeV	8 MeV	13 MeV	1 MeV(unfolding)	10 MeV

## ➤ Cross section measurement in each $M(K\bar{K})$ interval

$$\frac{d\sigma(K^+K^-)/dM(K^+K^-)}{\epsilon \cdot d\mathcal{L}_{\text{int}}/dM(K^+K^-)} = \frac{dN_{\text{sig}}/dM(K^+K^-)}{d\mathcal{L}_{\text{int}}} = w(s, x) \cdot \mathcal{L}_{\text{int}}$$

## ➤ Branching fraction measurement of $J/\psi \rightarrow K\bar{K}$

- Cross section for ISR production of a narrow resonance (vector meson  $V$ ), such as  $J/\psi$ , decaying in the final state  $f$  can be calculated by:

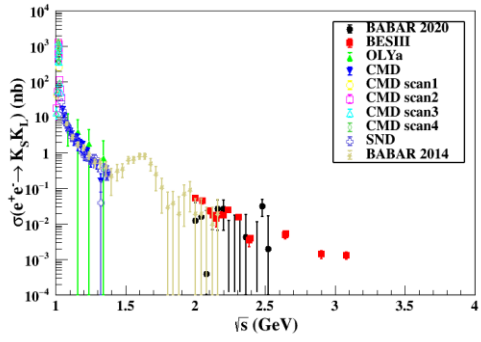
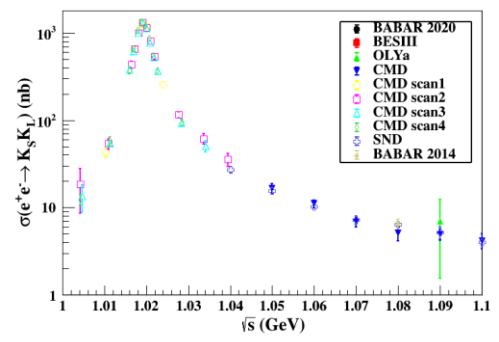
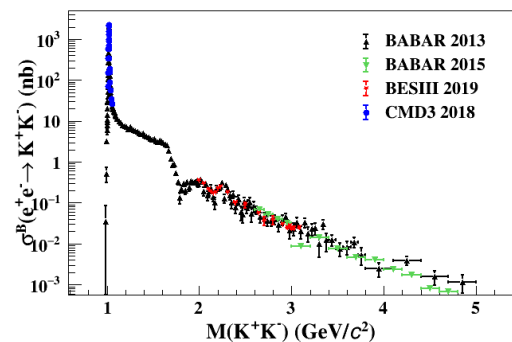
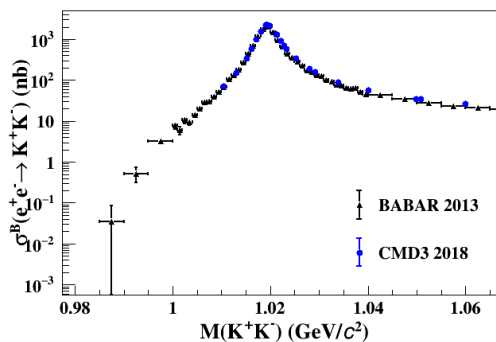
$$\sigma(s) = \frac{12\pi^2 \Gamma(V \rightarrow e^+e^-) \mathcal{B}(V \rightarrow f)}{m_V s} W(s, x_0) = \frac{N_{J/\psi}}{\epsilon \cdot \mathcal{L}} \quad \text{Experimentally}$$

Mod. Phys. Lett. A 14, 2605(1999)

# $K\bar{K}$ cross section

- Accuracy can be obtained at BESIII with  $20 \text{ fb}^{-1}$  datasets at  $\psi(3770)$  and  $10 \text{ fb}^{-1}$  datasets at XYZ region

Strategy	ISR Method(%)	Energy Scan Method(%)	ISR Method(%)
$e^+e^- \rightarrow K^+K^-$	Most accuracy results(statistical uncertainty only)		BESIII expected
Around $\phi$ peak	1.4 	0.3 	1.0
1.2 – 2.0 GeV	2.2 		1.5
2.0 – 3.2 GeV	10.0 	0.9 	4.5
$e^+e^- \rightarrow K_SK_L$	Most accuracy results(statistical uncertainty only)		BESIII expected
Around $\phi$ peak	2.2 	1.7 	1.2
1.2 – 2.0 GeV	14.0 		8.2





# Summary

- Measurements of  $e^+e^- \rightarrow K\bar{K}$  cross section via Initial State Radiation method are performed at BESIII with the large datasets(20  $\text{fb}^{-1}$  datasets at  $\psi(3770)$  and 10  $\text{fb}^{-1}$  datasets at XYZ region)
  - $e^+e^- \rightarrow K^+K^-$  with a tagged ISR photon
  - $e^+e^- \rightarrow K^+K^-$  with an untagged ISR photon
  - $e^+e^- \rightarrow K_SK_L$  with a tagged ISR photon
- High precision results will be obtained
- More results will come soon ...

Thank you !